Molecular Crystals and Liquid Crystals
Publication details, including instructions for authors and subscription information:
http://www.tandfonline.com/loi/gmcl16

Ferroelectric Liquid Crystal Electro-Optics Using the Surface Stabilized Structure

N. A. Clark [a] , M. A. Handschy [a] & S. T. Lagerwall [a b]
[a] Department of Physics, University of colorado, Boulder, Colorado, 80309
[b] Department of Physics, Chalmers University of Technology, S-41296, Göteborg, Sweden
Version of record first published: 21 Mar 2007.

To cite this article: N. A. Clark , M. A. Handschy & S. T. Lagerwall (1983): Ferroelectric Liquid Crystal Electro-Optics Using the Surface Stabilized Structure, Molecular Crystals and Liquid Crystals, 94:1-2, 213-233

To link to this article: http://dx.doi.org/10.1080/00268948308084258

Mol. Cryst. Liq. Cryst., 1983, Vol. 94, pp. 213–234
0026-8941/83/9402–0213/$18.50/0

Printed in the United States of America

Ferroelectric Liquid Crystal Electro-Optics Using the Surface Stabilized Structure

N. A. CLARK, M. A. HANDSCHY and S. T. LAGERWALL*

Department of Physics, University of Colorado, Boulder, Colorado 80309

The strong linear coupling of the director $\hat{n}$ to electric field E in ferroelectric liquid crystals can be utilized to perform high-speed electro-optic switching suitable for device applications. In this article we summarize the current understanding of the high-speed, bistable, threshold-sensitive electro-optic effects obtained in planar structures using surface interactions to suppress the spontaneous director helix characteristic of the bulk ferroelectric liquid crystal.

I. INTRODUCTION

Technical applications of liquid crystals still almost exclusively use nematics or chiral nematics, with smectic A thermo-optical displays now being introduced. Among the smectics, however, certain phases (the chiral tilted smectics) are ferroelectric, a property that offers a strong linear coupling of molecular orientation to an external electric field. Since 1974, when the first ferroelectric liquid crystals were reported by Meyer *et al.*,[1] the great potentialities of these new phases have been generally recognized, and extensive investigations on their electric properties and electro-optic response have been performed. This work has been reviewed by Meyer[2] and by Durand and Martinot-LaGarde.[3]

In 1980, a new ferroelectric smectic device structure, the Surface Stabilized Ferroelectric Liquid Crystal (SSFLC) structure, was reported,[4–6] showing that a very fast, bistable, electro-optic response with threshold is achievable in ferroelectric liquid crystals. In this article, we review the physics of SSFLC devices and describe some recent results on simple device structures.

*Permanent address: Department of Physics, Chalmers University of Technology, S-41296 Göteborg, Sweden.

II. SSFLC STRUCTURE AND PROPERTIES

All tilted smectics (C, F, G, H, I, ...) which are in addition chiral, are ferroelectric. The most fluid of these phases is the chiral smectic C, or C* for short. In an attempt to analyze how to achieve useful electro-optic response, let us first discard the chirality and look at a well-ordered C phase, where the molecules not only have a well-defined tilt angle θ, but also tilt in the same direction in space, given by an azimuthal angle ϕ, around the layer normal. Whereas θ is a function of temperature and shows normal fluctuations characteristic for a thermodynamic variable, the gauge invariance of the smectic C means that the phase variable ϕ can be freely varied (unlike θ it does not appear in the free energy), giving the C phase a nematic-like variable, ϕ. If now the smectic is chiral, it will be ferroelectric, the polarization density, $\mathbf{P}$, being locally perpendicular both to the molecules ($\hat{n}$) and the layer normal ($\hat{z}$). An external field, $\mathbf{E}$, lying *in* the layer can thus easily act on the variable ϕ and rotate the molecules. This yields a direct coupling of $\mathbf{E}$ to ϕ which is linear in $\mathbf{E}$. For time varying fields the response of ϕ is governed by a characteristic time τ given by $\tau^{-1} = \mathbf{P} \cdot \mathbf{E}/\eta$, where η is the orientational viscosity. The potential possibilities for new electro-optic applications can be judged from the fact that the rotational viscosity η is of the same order of magnitude as in a nematic, whereas for electric field magnitudes of interest, the product $\mathbf{P} \cdot \mathbf{E}$ can be made several orders of magnitude higher than the corresponding dielectric interaction energy in the nematic.

A side effect of the molecular chirality necessary for ferroelectricity in tilted smectics is a spontaneous local twist and bend deformation of the director, which induces a long pitch helical director structure characterized by a linear variation of ϕ with distance along the normal to the layers. A variety of electro-optic effects based on the electric field induced unwinding of this spontaneous helix have been reported.[2,3,7] An essential feature of any field induced helix unwinding, however, is the generation of topological defects (disclination walls) which must travel distances large compared to the pitch length to be eliminated from the sample. This leads to switching dynamics with relatively slow response, comparable to that of nematics. On the other hand, if ferroelectrics were helix-free, the electro-optic response could be a simple local reorientation and a high speed switching characterized by the relaxation time τ, as noted above, could be achieved. In the SSFLC structure, surface interactions are used to unwind the spontaneous helix.

The basic SSFLC structure[4–6] combines three appropriately chosen features (sample thickness, layer direction, boundary conditions), and is shown in Figure 1. The ferroelectric smectic is the dielectric in a trans-

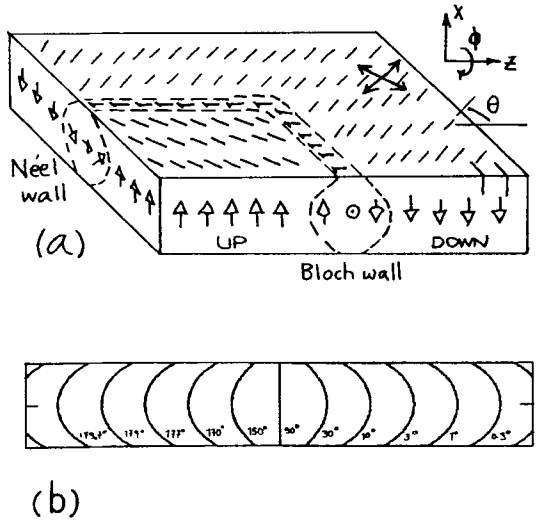

FIGURE 1 a) Schematic of the Surface Stabilized Ferroelectric Liquid Crystal Structure, showing the tilted smectic with layers normal to the bounding plates, the director orientation, $\hat{n}$ (short lines), and the accompanying ferroelectric polarization, **P** (arrows). The bounding plates are treated to constrain the director to be parallel to their surfaces, but free to reorient in the surface plane. The result is two stable states of the director field labeled here as UP and DOWN, according to the orientation of **P**. The displayed structure has both states present, separated by a domain wall, which in analogy to ferromagnets, is a Neél wall where it runs normal to the layers and a Bloch wall where it runs along the layers. b) Contours of constant orientation resulting from the continuum calculation of SSFLC domain wall structure presented in Section IV.

parent capacitor made from parallel, conductively-coated glass plates. The layers are oriented *perpendicular* to the glass plates so that the electric field vector is in the plane of rotation of **P**. In this geometry the helix can be "elastically unwound" if the sample surfaces are treated to enforce any particular director orientation, and if the sample thickness is made small enough—of the order of the helical pitch, which is commonly a few microns. If, for example, the boundary conditions are now chosen such that the molecules have a preference to align parallel to the bounding glass plates, the result of the combined constraint on the molecules at the surface to lie on the tilt cone, and simultaneously in the surface will result in two preferred, distinct (but structurally equivalent) director orientations. We denote these two stabilized states by UP and DOWN or by $+\mathbf{P}$ and $-\mathbf{P}$, as indicated in Figure 1. Switching from one state to the other is achieved by reversing the direction of the applied field (see Figure 1). Because these are stabilized states, adjacent regions of opposite orientation will be separated from each other by distinct boundaries, as illustrated in Figure 1, which,

in analogy with similar structures in crystalline ferroelectrics and ferromagnets, we call domain walls. However, a clear distinction can be drawn between SSFLC domain walls and those found in crystals: SSFLC walls are stabilized by surface interactions and not by bulk crystal anisotropy. Indeed, deGennes and Pincus have shown that domain walls are not possible in the bulk in a variable with continuous orientational degeneracy such as ϕ in a C*[8]. Pursuing the magnetic analogy further, the domain walls are "Bloch-like" if directed along the smectic layers, and "Neel-like" if normal to the layers (cf., Figure 1).

We now point out several unique and novel features of the SSFLC geometry. With the helix unwound, a ferroelectric smectic in the SSFLC geometry behaves optically essentially as a uniaxial slab with the uniaxis along the director orientation. The effect of switching is to rotate the uniaxis about the normal to the surface through an angle of twice the tilt angle θ. The SSFLC is the only liquid crystal parallel-plate geometry allowing a rotation of the uniaxis of a homogeneous sample about the surface normal. Another SSFLC feature to be noted is the nature of the required boundary condition. In order to obtain bistability, boundary conditions which constrain the molecules to be parallel to the plates, but allow several or continuous orientations about the normal to the plates are required. The SSFLC is the first liquid crystal electro-optic structure to employ such a combination of strong-weak boundary conditions. A consequence of this feature and an essential SSFLC property is that the director at the surfaces is switched between stable surface orientation states as an essential part of the overall switching process. The SSFLC is the first liquid crystal electro-optic structure to successfully employ multistate surfaces and the only structure wherein switching between stable surface states has been demonstrated.

III. SSFLC OPTICAL PROPERTIES

SSFLC switching involves a substantial director reorientation which can be exploited to produce a variety of optical effects. We limit our discussion here to the simplest situation of sandwiching the SSFLC cell between crossed polarizer and analyzer and deriving optical contrast from the homogeneous uniaxial birefringence of the SSFLC slab. Apart from factors depending on the quality of the surface treatment, polarizers, and so on, the optical transmission of a SSFLC slab between polarizer and analyzer is determined by the relative orientation of the polarizer, analyzer and the uniaxis, $\hat{n}$, as is the case for any smectic A or C fan texture.

This is illustrated in Figure 2, which shows a smectic A focal conic fan texture (DOBAMBC,[1,4] thickness = 1.5 μm) between crossed polarizer (vertical) and analyzer (horizontal) exhibiting extinction brushes wherever $\hat{n}$ is horizontal. The orientation of $\hat{n}$ can be determined in some areas from the orientation of the curved extended dark stripes which are air bubbles in the preparation, the long surfaces of which run parallel to the smectic layers; where the stripes are locally vertical, the smectic A director is horizontal and the smectic A extinct. The sample of Figure 2b has been subjected to a gentle shearing of the glass bounding plates relative to one another in the vertical direction, a process which rotates the layers into that direction. The confocal domains are now much extended horizontally, running roughly normal to the layers. This picture shows clearly the increased optical transmission accompanying the local rotation of the layers away from the vertical. Of particular note in Figure 2b is the sensitivity of optical transmission to orientation for this geometry. Extinction occurs only for a small range of orientation of $\hat{n}$ about the horizontal. This effect is well known as "flash figure or flash extinction" in the optical crystallography of uniaxial crystal slabs having the uniaxis parallel to the slab. For the SSFLC, this implies that good optical contrast can be achieved even for ferroelectrics with tilt angles as small as a few degrees. For thin samples this excellent optical contrast is achievable over a large cone of incident light directions.

SSFLC birefringence contrast effects are illustrated in Figure 3, where the focal conics are roughly vertical (Figure 3a), corresponding to shear and layers horizontal (Figure 3b). The ferroelectric $+\mathbf{P}$ and $-\mathbf{P}$ domains are here clearly visible appearing in Figure 3a with comparable brightness because the tilt directions in both are at about the same inclination to the polarizer direction. The domains are separated by walls, which show up dark because, in going from $+\mathbf{P}$ to $-\mathbf{P}$, $\hat{n}$ rotates through an extinction angle. The domain walls are about 2 μm wide, which is comparable to the sample thickness, as discussed in Section IV. When turning the sample or the polarizers in either direction, one domain is brought into further extinction, the other to further transmission and thus contrast appears as in Figure 3c. The highest contrast will appear when polarizer and tilt direction coincide for one domain, for which we will ideally have perfect extinction, whereas a fraction $\sin^2(4\theta) \cdot \sin^2(\pi n_a d/\lambda)$ of the intensity will be transmitted through the other domain. This fraction can be made near one, but is generally a function of temperature, T, because θ depends on T, and is also a function of the refractive index anisotropy, n_a, and the thickness of the cell, d. A high value of n_a, *e.g.*, $n_a = 0.25$ would be typically optimized by a thickness $d = 1$ μm (at 0.5 μm light wavelength), with the

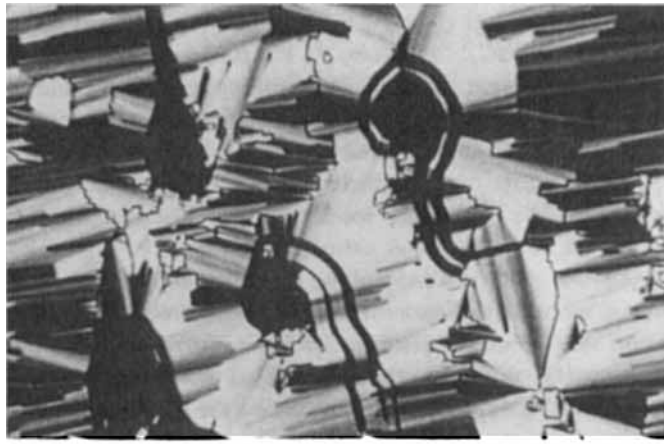

a

b

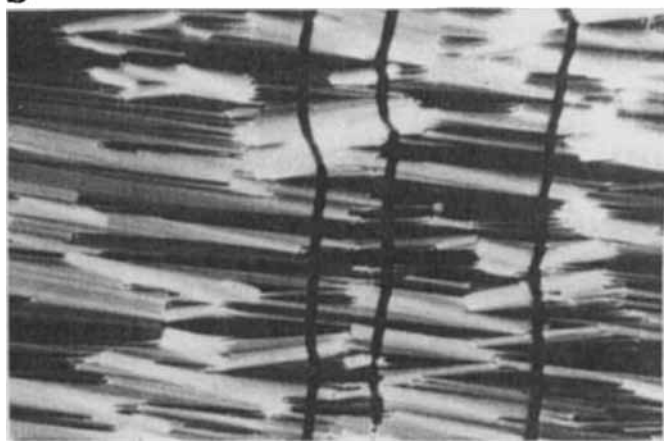

FIGURE 2 a) Smectic A focal conic texture of a 1.5 μm thick DOBAMBC[1] sample between clean ITO coated glass plates viewed in transmission between crossed polarizers (field width = 320 μm). The focal conics are interrupted by elongated bubbles which run parallel to the layers, indicating their local orientation. Extinction occurs for the layers either vertical or horizontal. b) Sample after a small relative displacement of the plates in the vertical direction. The layers reorient to run generally along the shear (vertical) direction. The vertical dark line is an extended bubble, and indicates the local layer orientation, as in *a*). Notice the high sensitivity of sample transmission to layer orientation in this geometry, with significant transmission occurring for only a few degrees orientation away from the vertical. This leads to useful SSFLC birefringence-based electro-optic effects even for small tilt angle, θ.

These figures appear in full color at the back of the journal.

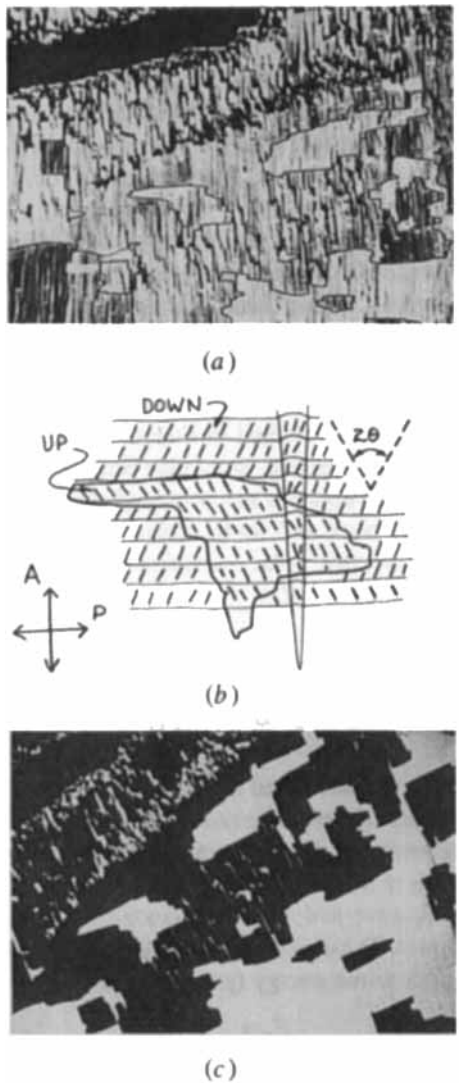

FIGURE 3 a) SSFLC domains in a 1.5 μm thick smectic C* DOBAMBC sample between clean ITO coated glass plates. The layers have been partially ordered into the horizontal direction by weak shear, with remnant focal conics giving the vertical texture (image field width = 320 μm). With this orientation, UP and DOWN domains have the same transmission as the director makes the same angle with the polarizer in both. Because the director rotates through an extinction band upon passing through a domain wall, they show up as dark lines. The domain walls are sharp, about 2 μm thick, indicating a surface interaction length that is small compared to the sample thickness. b) Schematic indication of director orientation in the domain just left of center in *a*). c) Sample in *a*), rotated to extinction of the DOWN domain.

optimum d varying as $1/n_a$ for other materials. We will return to the discussion of this and similar material considerations in the last section.

Whereas the achievable contrast is potentially the same as for the twisted nematic display, there is one important difference in aspect: in this case a birefringence effect is used, hence we can switch not only between black and white (or black and one color) but between two different colors, depending for a certain sample thickness only on the setting of the polarizers.

Oppositely switched states are illustrated in Figure 4. Here a cylindrically shaped confocal domain (with the typical split of the central +1 disclination into two +½ disclinations) is acted upon by an electric field, turning the molecules around the cone axis into the opposite position in the paper plane. The director is switched by the angle 2θ and the four extinction brushes are rotated by the same amount. This mechanism, thus, also gives a very simple method of directly measuring the tilt angle as a function of temperature or, *e.g.* substance composition in mixtures. Due to the linear interaction between the polarized medium and the field, these brushes will rotate back and forth, following the polarity changes in an applied AC voltage; this polar switching mode is principally absent in non-ferroelectric liquid crystals.

IV. THE STRUCTURE AND MOTION OF DOMAIN WALLS

We now consider in more detail the SSFLC domain wall structure and the dynamical behavior of molecular reorientation in the presence of an applied time varying electric field. We begin by calculating the equilibrium structure of the Bloch π domain wall of Figure 1, which, in the absence of an electric field, is governed by the balance of Frank elastic and surface interaction torques. The observed planar surface interaction can be modeled most simply with a free energy (per unit area),

$$F_s = -\Delta\gamma\cos^2\phi\,.$$

The distortion free energy (density) for a chiral smectic C includes terms due to the variation in interlayer distance, variation in the tilt angle, θ, and variation in the "C director", the projection of $\hat{n}$ onto the smectic layer plane. Fixing the first two contributions, which are substantially larger than the third, at their minimum values, the distortion free energy is, to within a constant

$$F_d = \frac{1}{2}K_1(\nabla\cdot\hat{n})^2 + \frac{1}{2}K_2(\hat{n}\cdot\nabla\times\hat{n}) + q_\parallel)^2 + \frac{1}{2}K_3(\hat{n}\times\nabla\times\hat{n} + \mathbf{q}_\perp)^2\,.$$

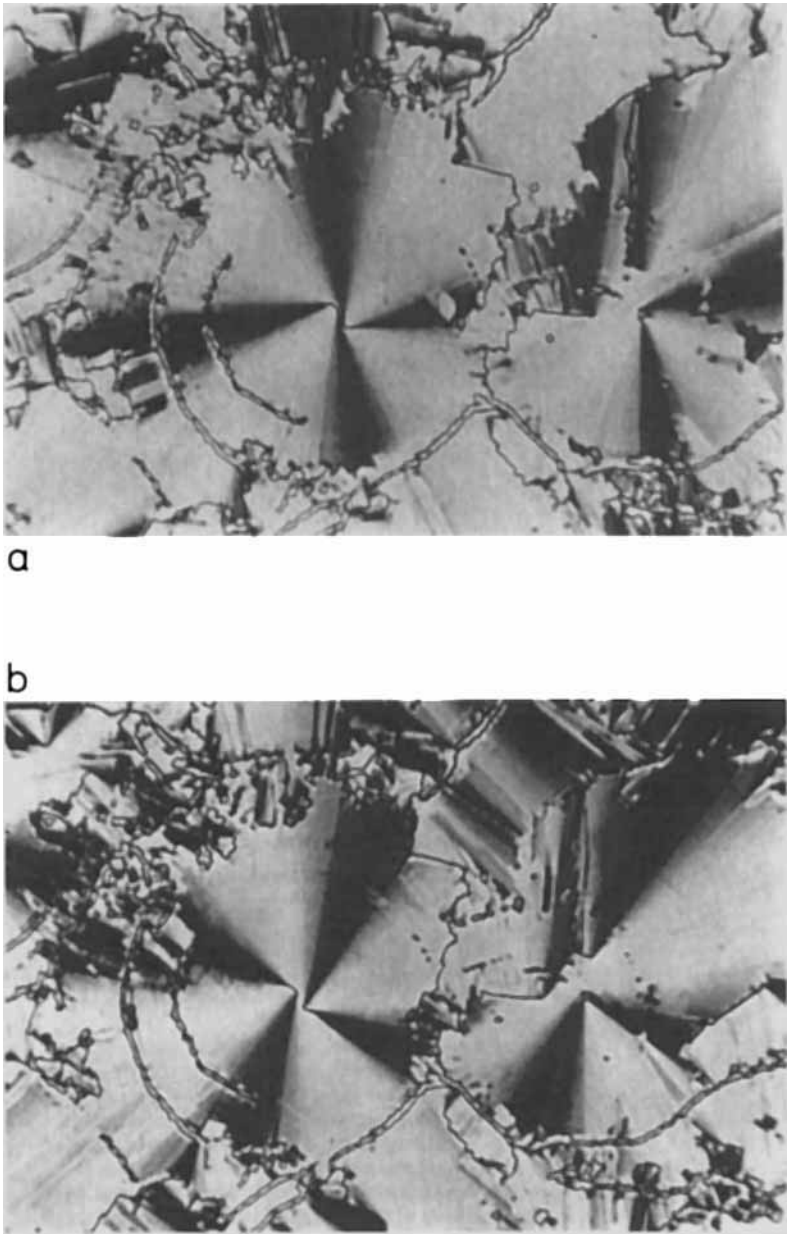

FIGURE 4 Nearly cylindrical focal conic domain in a 1 μm thick smectic C* DOBAMBC sample (field width = 320 μm). a) DOWN state. b) UP state. The angle between the brushes in *a*) and *b*) is twice the smectic tilt angle, θ.
These figures appear in full color at the back of the journal.

In the one-constant approximation, this simplifies to

$$F_d = \frac{1}{2}K(\nabla\phi)^2 + Kq_b(\sin\phi\phi_x - \cos\phi\phi_y) + Kq_t\phi_z,$$

where the wave vector of "twist" of the C-director is

$$q_t = q_\parallel + |\mathbf{q}_\perp| \cot\theta,$$

and the wave vector of "bend" of the c-director is

$$q_b = q_\parallel \cot\theta + |\mathbf{q}_\perp|.$$

Minimization of the total free energy,

$$f = \int F_d \, dV + \int F_s \, dA,$$

yields, by way of the Euler-Lagrange equation, the Laplace equation $\nabla^2\phi = 0$, and the surface condition

$$K\phi_x \pm \Delta\gamma \sin 2\phi = 0, \tag{1}$$

where the plus sign is taken at $x = d$ and the minus sign at $x = 0$.

Now, looking for a straight domain wall, without loss of generality parallel to the y-axis, take $\phi_y = 0$. Further, a π-wall centered at $z = 0$ has $\phi(x, z = \infty) = 0$, $\phi(x, z = -\infty) = \pi$, $\phi(x, z = 0) = \pi/2$. This problem has the solution

$$\phi(x,z) = \tan^{-1}\left\{\frac{\sin\dfrac{\pi(x+s)}{d+2s}}{\sinh\dfrac{\pi z}{d+2s}}\right\}, \qquad 0 \le z < \infty$$

$$\phi(x,z) = \tan^{-1}\left\{\frac{\sin\dfrac{\pi(x+s)}{d+2s}}{\sinh\dfrac{\pi z}{d+2s}}\right\} + \pi, \qquad -\infty < z < 0$$

where s is a solution of

$$\tan\frac{\pi s}{d+2s} = \frac{K\pi}{2\Delta\gamma}\frac{1}{d+2s}.$$

Constant director orientation contours for this solution are plotted in Figure 1b. The surface interaction is characterized by a length, $l_s \equiv K/\Delta\gamma$. For weak surface interactions, $l_s/d \gg 1$, and the domain wall "width" is comparable to $s = \pi/4 \cdot \sqrt{l_s d} > d$. For strong surface interactions,

$l_s/d \ll 1$ and $s \approx 2l_s$. In this case, the domain wall width is comparable to the sample thickness, d. Infinite surface interaction strength gives $s = 0$. This case has the simpler boundary condition, $\phi(z > 0) = 0$ and $\phi(z < 0) = \pi$. For $z \geq 0$, this is equivalent to the two-dimensional electrostatic problem of determining the electrostatic potential in a semi-infinite strip bounded by grounded conductors. Since Laplace's equation is linear, the solution is obtained by the usual method of superposition, and the resulting fourier series can be summed to give the solution stated above with $s = 0$. Recent measurements on DOBAMBC samples with clean ITO surfaces[9] and $d \approx 1$ μm indicate $l_s = 0.13$ μm, exemplifying the case of relatively strong surface interactions, in which case the wall thickness should be roughly equal to the sample thickness. Figure 3a, where the polarizer setting is such that the wall itself gives extinction contrast against the adjacent domains, is an illustration of this: the thickness of the walls can be seen directly to be $\simeq 2$ μm, corresponding to the sample thickness of $\simeq 1.5$ μm.

The dynamical behavior of $\phi(x, y, z)$ in response to time varying applied electric fields may be calculated using field equations incorporating the electric field and viscous torques along with the surface and elastic torques. The result is a nonlinear second order differential equation for $\phi(x, y, z, t)$, with the nonlinear boundary condition of Eq. (1). We have not succeeded in obtaining solutions for these equations except for simple situations (*e.g.*, the spatially uniform case), but our experimental studies have enabled us to develop a qualitative picture of the main features of the switching dynamics in various fields and time regimes. The scaling parameters governing this behavior are the surface length, l_s, discussed above, the bulk elastic-field scaling length, $\zeta = \sqrt{K/PE}$, the sample thickness, and the relaxation time $\tau = \eta/PE$. In the case discussed above ($l_s \ll d$), three electric field regimes have been established.[9,4]

LOW FIELDS — Low field behavior occurs when $\zeta > d$. Since the length ζ is the distance required by the competition of electric and Frank elastic torques for reorientation to occur, the field in this regime is not large enough to appreciably distort the equilibrium domain wall structure. In the absence of pinning sites an applied field will move the walls with a velocity $v \simeq PEd/\eta$. In practice, there are many pinning sites on which, in the presence of a slowly increasing DC field, the walls will locally hang up and then pop off. This can be seen in the sequence of Figure 5, where an increasing electric field causes one type of domain to grow at the cost of the other one until domains from several nucleation centers ultimately coalesce. Figure 5e shows a particularly striking example of pinning, with a long horizontal extension of the dark domain being maintained by two strong pinning sites (unidentified). Because of this pinning, switching is

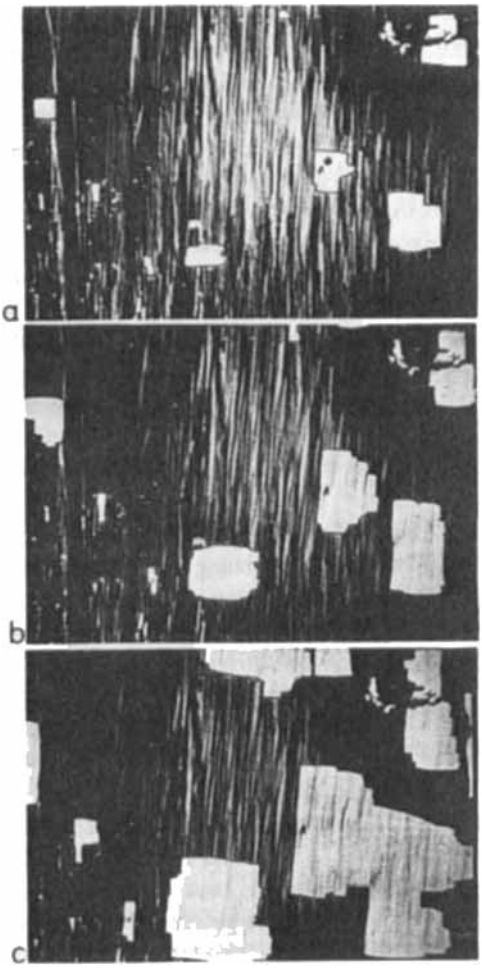

FIGURE 5 A sequence of SSFLC domains in a 1.5 μm thick smectic C* HOBACPC[4] sample showing domain wall motion in the LOW field regime in response to a slowly increasing voltage of 0V (a) to 1.5V (f). The moving domain walls encounter pinning sites which are successively overcome as E is increased. In e) the narrow extension of the dark domain to the right is caused by a pair of strong pinning sites impeding wall motion (image field width = 320 μm).

not possible for field pulses below some minimum amplitude ($\simeq 10^3$ V/cm).

INTERMEDIATE FIELDS — Intermediate field behavior occurs when $l_s < \zeta < d$. In this case the application of a field step produces director reorientation in the center of the sample in time, τ, leaving, on each

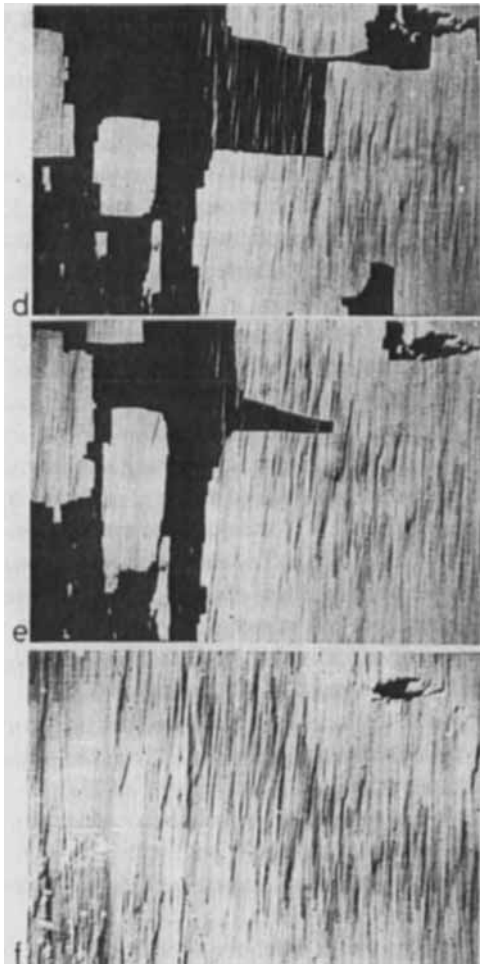

FIGURE 5 (continued)

surface, layers of thickness ζ having the original orientation. These surface disclination walls are stable against a reorientation that is uniform over the whole surface because, with $l_s < \zeta$, the field is not strong enough to homogeneously overcome the surface anchoring. However, surface reorientation can occur inhomogeneously by the nucleation and growth of switched domains in this surface layer. Bistable latching in response to a voltage pulse occurs once these surface domains form and spread sufficiently over the surface to percolate and form connected regions of the

switched surface state. Hence, in this case, switching response time depends on the nucleation density and velocity of these surface domains. Stroboscopic microscopy shows that the surface domain wall velocity increases approximately linearly with E ($v \simeq 1$ cm/sec for $E \simeq 10^5$ V/cm).

HIGH FIELDS — High field behavior occurs for $\zeta < l_s$. In this limit the surface disclination wall distortion becomes so tight that the torques applied to the surface are large enough to overcome the surface energy barrier and homogeneously reorient the surface. The director responds almost as if the medium were infinite and spatially uniform, exhibiting the response time τ.

Quantitative studies of the time dependence of SSFLC optical transmittance in response to rectangular electric field pulses is summarized in Figure 6. The specimen is HOBACPC in the C* phase at $T = 68°C$ and $d = 1.5$ μm. Alternate plus and minus pulses of 1.4 μs duration are applied at 70 ms interval (Figure 6a, top curve) and the optical transmission of the SSFLC between crossed polarizers is monitored by a photodiode (Figure 6a, lower curves). It is seen that the switching does not occur at a pulse height of 26 volts. To get bistable operation we would, in this case, have to increase the pulse width to about 2 μs. If we instead keep the width constant as is illustrated, the monostable operation will start to change its character visibly at about 30 volts. Hereafter the pulse begins to "latch" the monitored area which stays in the switched position. This latching is complete at about 35 volts. From then on the cell stays in the UP state until it is switched DOWN by the pulse following 70 ms later. This example shows that bistable operation is achievable at high switching speed and even with a fairly sharp threshold. Notice that the memory (at least of the order of secs) is far more than sufficient for the addressing of the elements in a video or computer terminal screen which only require updating about every 30 ms.

Figure 6c shows the pulse width required to produce bistable latching for rectangular pulses of amplitude V, according to the discussion just given. The specimen is HOBACPC in the C* and F* phase and the sample thickness 1.5 μm. The three different field regimes can be observed. In the LOW field limit ($V < 0.1$ Volts), there is no bulk switching at all, because the field cannot nucleate or unpin domain walls. In the INTERMEDIATE field regime the latching time is governed by the overlap of surface domains. As the field increases, the surface domains nucleate sooner, in greater number and sweep the sample faster, leading to a strong dependence of latching time on the applied field (varying nearly as E^{-2}). As the field increase continues, however, also the thickness of the unreversed domains in the x direction decreases, finally below the significant level for optical

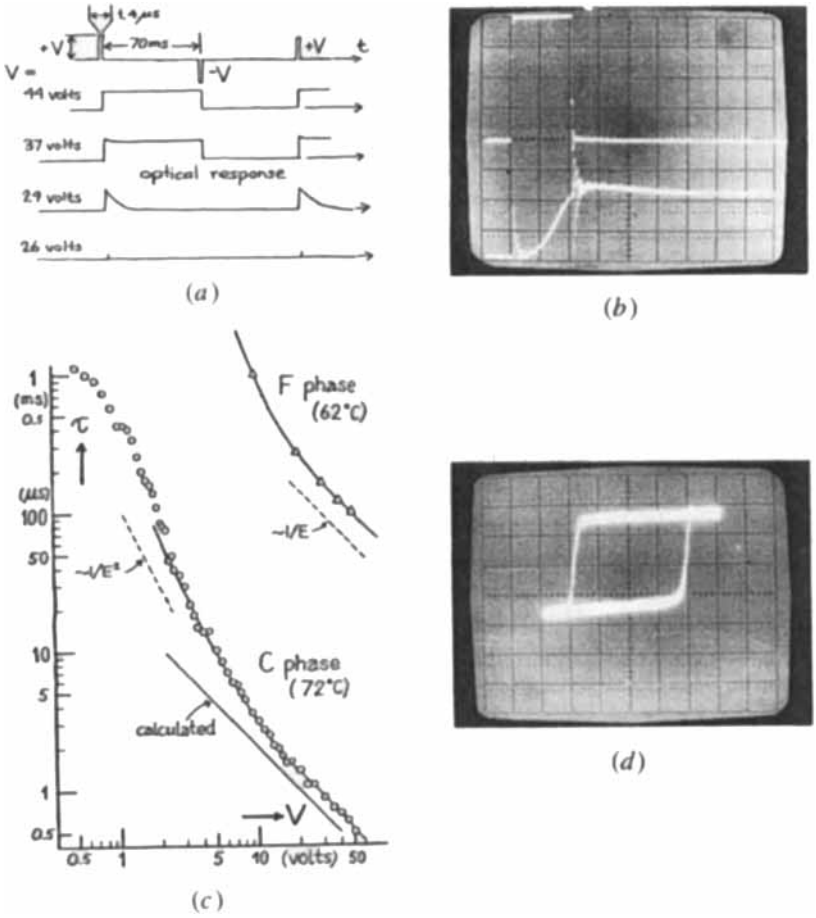

FIGURE 6 Electro-optic response of a 200 μm^2 area of an SSFLC device employing a 1 μm thick smectic C* HOBACPC layer at $T = 68°C$ between clean ITO plates. a) The top trace shows the applied train of 1.4 μsec long pulses. The lower traces show the response of the optical transmission for increasing pulse amplitudes, indicating a sharp threshold for switching at about 30 V. Optical transmission in the latched state is that for a uniformly oriented sample. b) Detail of the optical transmission response (lower trace) for a 40 V, 1 μsec long pulse (top trace). Horizontal scale is 500 nsec/div. c) Pulse amplitude required for latching as a function of pulse width for the C* and F* phases. See text for a discussion of the various regimes. d) Hysteresis loop obtained with a slowly varying triangle wave. Vertical axis is optical transmission and the horizontal axis scale is 0.5 V/div.

contrast. We then enter the regime of HIGH fields where the switching proceeds nearly as in the bulk, with the required latching time very nearly $\tau = \eta/PE$.

Figure 6b shows a single pulse (width = 1 μsec, amplitude = 40V) and the optical response with a 0.5 μsec risetime, the shortest yet observed. This response time is no limit *per se;* by careful design of molecules, new materials with lower η and higher P are likely to be synthesized. For any one material, τ can be made smaller by increasing E, the limit for the switching speed thus being set by the dielectric or chemical breakdown of the material in question and by the RC time constant of the electrode-liquid crystal capacitor.

Generally for bulk switching including relaxation from some elastic distortion (of wave vector $\mathbf{k}$) τ is given by

$$\tau^{-1} \approx (K\mathbf{k}^2 + E \cdot P)/\eta$$

which is connected with the dimensions of the sample or, if the helix were present, with the pitch. In our high field limit the first term is negligible relative to the second one. For E small, τ is determined by $\mathbf{k}$, which gives a relaxation time typically of the order $\geq$1 ms. This "zero field" value, which also fairly well corresponds to the measured relaxation frequencies of 1 kHz or less[12] can be considered as the minimum memory time for ferroelectric switching. For very high speed applications, 1 ms is still a long time compared to the shortest switching time of less than 1 μs. Thus, the elastic relaxation back in zero field may serve as the simplest short term memory mode in these materials.

For other applications, when essentially permanent memory is required, one might instead use switching of the ferroelectric F* phase. The F* phase possesses considerably more interplanar translational order than the C* phase ($\simeq$100 molecules in local crystalline correlation areas), resulting in an orientational viscosity and switching response time which is about 100 times that of the C*. The switching is, however, still rapid enough for many applications (see Figure 6c), and the memory effects are pronounced. An oscilloscope trace of the electro-optic hysteresis loop in such a case is shown in Figure 6d. Again, it shows the change in the transmittivity of the cell (DOBAMBC in the F phase between crossed polarizers) as monitored by by a photodiode (photodiode response along y-axis). The applied voltage (along x-axis) is a growing pulse of triangular shape and its inversion, with 4 volts peak to peak and a repetition frequency of 0.1 Hz. It is seen that the transmission characteristic is quite non-linear, displaying both a relatively sharp switching threshold and further saturation and memory behavior. The shape of the hysteresis loop also shows that the bistable operation is *symmetric* with regard to the plus (lower-right) and the minus (upper-left) pulse. The principal features in this essentially DC response remain, upon going to higher frequencies.

V. SIMPLE DEVICES

So far we have reported only on measurements and observations made on samples characterized primarily by confocal domains having the layers forming sets of nested cylinders normal to the surface plates, where only small parts have been well-aligned enough to be useful for the monitoring of switching. In order to make devices, layer alignment, sample thickness, and surface conditions have to be better controlled. Some steps toward this goal will now be reported.

We have designed a matrix addressed cell geometry with the ferroelectric liquid crystal between glass plates — a 32 × 32 element array of 300 μm square pixels — made by photolithographically preparing arrays of ITO strips on the plates and arranging the strips on the opposite plates to be mutually perpendicular. The glass plates, which were either 25 mm wide microscope slides (1 mm thick) or cover slips (0.15 mm thick), were first covered with a conductive ITO coating (500 Å thick, 50 Ω/sq) which was then etched into strips, 300 μm wide with 30 μm wide gaps in between. Along the edge of each strip an aluminum lead was evaporated (1000 Å thick, 20 μm wide) in order to reduce the series resistance to the pixels. Between the ITO strips were evaporated SiO spacer strips, typically of 30 μm width and 1 μm thick. SiO spacer strips and pads have been successfully used to establish uniform spacings in the range of 0.25 μm to 2 μm in our cells. Mechanical or hydrostatic pressure is used to press the plates together, against the spacer array, obviating the need for optically flat plates.

Single plates prepared in this way were used to make stripe cells by clamping a plain ITO coated glass plate on top of the striped plate, pressing against the underlying spacers, and filling the cell with the ferroelectric liquid crystal. The 1 μm thick LC sample was now aligned in the A phase by applying a very gentle AC shear to the sample by moving the bottom glass plate relative to the top. Typical shear rates are from 1 to 10 Hz, with a maximum relative displacement amplitude of about 20 μm. Both the SiO spacers and the ITO coating are hard enough to permit the shearing motion, even when a reasonable pressure is applied across the glass plates. The shear, a more refined and controlled version of what is mentioned in Section III, has to be performed in the highest range of the A phase (typically about 2–5°C below the transition to isotropic liquid) in order to have the viscosity reasonably small, and aligns the smectic A layers to a high degree. The layers stay fixed when going down in the C phase.

The action of the shear is certainly very complicated in detail, but the following simple considerations can be made. If we consider the surfaces

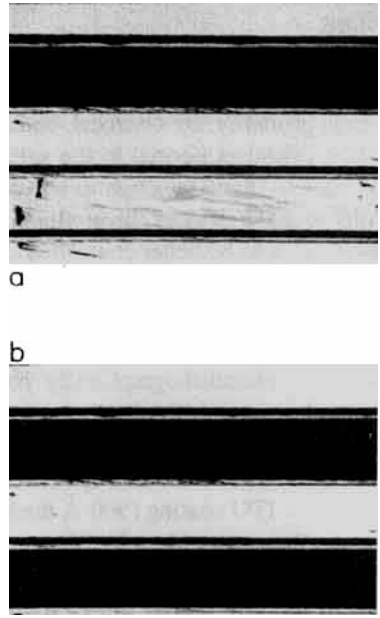

FIGURE 7 a) A 1 μm thick smectic C* DOBAMBC SSFLC stripe cell with one stripe switched off. The ITO stripes, etched on one of the plates (a microscope slide), are 300 μm wide and 30 μm apart. The other plate is an ITO coated microscope cover slip. The yellow-white color is the birefringence color of the 1 μm thick DOBAMBC. The 30 μm wide black line at the edge of each stripe is the aluminum conductor. The blue lines are the 30 μm wide, 1 μm thick SiO spacing bars, which determine the sample thickness. The smectic layers run vertically, having been ordered by a shear of the plates in that direction. The smectic layer order is essentially perfect. Stripe 3 is switched off in b).
This figure appears in full color at the back of the journal.

as unbiased, there are two, and only two, configurations in which non-permeative flow can occur under a weak shear. The first (1) has the layers perpendicular to the glass plates and parallel to the direction of shear. Thus, if we start with a confocal arrangement of perpendicular layers, these will tend to configuration (1) because it is a (local) minimum of dissipation. In most cases this configuration will be metastable and tend, when forced by a shear which is too large, to the configuration (2) where all layers are instead parallel to the glass plates (homoeotropic). If the starting surface conditions are such that the molecules prefer to lie parallel to the plane of the glass plates (which seems to be the case for clean ITO and many molecules), then the metastable situation (1) is at least somewhat stabilized relative to (2) and the desired alignment facilitated.

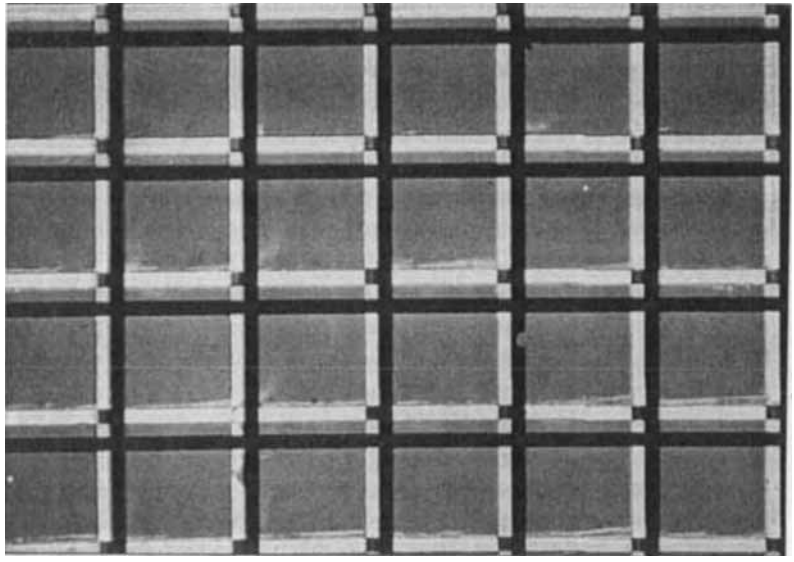

FIGURE 8 Smectic C* DOBAMBC between two stripe plates identical to that of Figure 7, each with aluminum conductors (dark lines) and 1 μm thick SiO spacer strips (yellow-white lines). The purple color is the birefringence color where the liquid crystal layer is 2 μm thick. The spacers appear yellow-white because the liquid crystal layer is only 1 μm thick under them. Where the spacers cross there is no liquid crystal and extinction occurs.
This figure appears in full color at the back of the journal.

The homogeneity of the alignment achievable in this way can be judged from Figure 7a and 7b, which also demonstrates the switching contrast. It is hardly possible to discern any reminiscences of the layered structure focal conics defects. The yellow-white birefringence color (for crossed polarizers) is characteristic of a 1 μm thick DOBAMBC sample.

In Figure 8 two identical stripe plates with SiO spacers have been crossed facing each other, making a matrix array. The black x-y lines in the figure are the non-transparent aluminum leads, the yellow-white x-y lines are the SiO spacers. Along a spacer, the smectic crystal is only 1 μm thick, hence the color. From glass to glass the smectic crystal is 2 μm thick and the purple color of each matrix element is the birefringence color corresponding to that thickness. Where the spacers cross, finally, there is no birefringent medium present. These crossings are therefore blackened out between crossed polarizers.

Although the alignment is still not quite perfect, as it can be seen in the micrographs, it gives confidence in the future use of these materials in display devices.

VI. CONCLUSION

Some of the problems and promises with the liquid crystal ferroelectrics as fast-switching media have already been discussed elsewhere[6] and will not be repeated here. Our comments below are an attempt to summarize what we think is the latest progress and assess the present situation.

Except for the unusual boundary condition and geometry, which have certainly never been used in any display devices (and are therefore correspondingly scarcely studied), the hardest problem to overcome was initially felt to be the necessity of maintaining the unusually small sample thickness, of about 1 to 2 μm, constant over a reasonable area. That this problem can be mastered by the technique of evaporation of the spacers should be immediately evident from Figure 7, where the constancy is translated in the desired homogeneity of the birefringence colors. If, on the other hand, for some applications it would be thought more convenient to use the more standard sample thickness of the order of 10 μm, it might be reminded that switching times of less than 5 μs can still be achieved with materials of present-day polarization density. Regarding achievable switching speeds and electro-optic performance, in general, it is clear that with the ferroelectric liquid crystals we are in a "PAA situation," corresponding to the nematic case about 15 years ago. The remarkable development in nematic synthesis since then, mainly due to British and German chemists, has been instrumental in providing the optimized materials (especially materials with drastically lower viscosity) used in today's displays. There is no reason why a similar future could not be expected for ferroelectrics, and developments such as the new room temperature compounds of the Chalmers and Bell Laboratories groups will hopefully point the way to a significant synthetic effort aimed at finding new and interesting ferroelectric liquid crystals. With lowered viscosity and higher polarization the present switching time limit of 500 ns might be able to be cut down to $\simeq$50 ns, with $\simeq$10 ns as an educated guess for the ultimate materials and structural limitations for liquid crystal switching in general.

In conclusion, some of the most important aspects of SSFLC switching can be summarized as follows:

1) It is rapid, in fact more rapid than any other switching mechanism in liquid crystals. The threshold is also generally sharper.

2) It is bistable, i.e., it has a storage mode, and the bistability is symmetric, which means it can be switched back and forth with the same speed by applying short pulses of opposite sign. This also means selective erase at the same speed.

3) It has essentially the same contrast possibilities as the twisted nematic device and an additional intrinsic capability of color switching.

4) a grey scale (or color scale) can be introduced in several ways, in particular by exploiting the high speed and pulse width modulation.

These properties suffice to make the ferroelectric liquid crystal an obvious future candidate in many areas where the limitations in speed presently present the greatest obstacle to be overcome in extending the technology of liquid crystal devices. It also makes the ferroelectric liquid crystals specially attractive for the development of simple modulation devices, or devices for real time processing of light (incoherent — coherent converters) or large non-emissive picture screens. Such screens would have an appealing simplicity and low cost because it obviates laser beam scanning or backing by non-linear elements, and could be addressed either by a conductive matrix coating or quasi-continuously in contact with a photoconductive layer.

Acknowledgments

This work has been supported by ARO, contract DAAG 29-79-C-0174, and by the Swedish National Board for Technical Development (STU). The authors are grateful for the use of the excellent photolithography facilities of the Laboratory for Superconducting Devices at the National Bureau of Standards in Boulder, CO, and wish to thank F. Lloyd, D. Doughty, and F. Hester for their technical assistance and advice.

References

1. R. B. Meyer, L. Liebert, L. Strzelecki, and P. Keller, *J. de Phys.*, **36**, L69 (1975).
2. R. B. Meyer, *Mol. Cryst. Liq. Cryst.*, **40**, 33 (1977).
3. G. Durand and Ph. Martinot-Lagarde, *Ferroelectrics*, **24**, 89 (1980).
4. N. A. Clark and S. T. Lagerwall, *Appl. Phys. Lett.*, **36**, 899 (1980).
5. N. A. Clark and S. T. Lagerwall, in *Liquid Crystals of One and Two Dimensional Order*, W. Helfrich and G. Heppke, Ed., Springer-Verlag, Berlin (1980) p. 222.
6. N. A. Clark and S. T. Lagerwall, in Recent Developments in Condensed Matter Physics, Vol. 4, J. T. Devreese, L. F. Lemmens, V. E. Van Doren, and J. Van Doren, Ed., Plenum, New York (1981) p. 309.
7. K. Yoshino and Y. Inushi, *Jap. Journ. Appl. Phys.*, **20**, Suppl. 20-4, p. 3 (1981); K. Yoshino, T. Uemoto, T. Urabe, and Y. Inushi, *Jap. Journ. Appl. Phys.*, **20**, Suppl. 20-4, p. 215 (1981).
8. P. G. deGenes and P. Pincus, *Sol. St. Comm.*, **7**, 339 (1969).
9. M. A. Handschy and N. A. Clark, *Appl. Phys. Lett.*, **41**, 39 (1982).
10. A. Hallsby, M. Nilsson, and B. Otterholm, Mol. Cryst. *Liq. Cryst. Lett.*, **82**, 61 (1982).
11. J. W. Goodby and T. M. Leslie, Presented at the Symposium on Ordered Fluids and Liquid Crystals of the 183rd American Chemical Society National Meeting, Las Vegas, Nevada (1982).
12. K. Yoshino, T. Uemoto, Y. Inushi, *Jap. Journ. Appl. Phys.*, **16**, 571 (1977); B. I. Ostrovsky, A. Z. Rabinovitch, A. S. Sonin, B. A. Strukov, *Sov. Phys. JETP, 47*, **5**, 912 (1978); J. Hoffmann, W. Kuczynski, J. Malecki, *Mol. Cryst. Liq. Cryst.*, **44**, 287, (1978); D. S. Parmar, Ph. Martinot-Lagarde, *Ann. Phys.*, **3**, 275 (1978).